

## Numerical modelling of transport in a liquid diffusion couple shear cell

This article has been downloaded from IOPscience. Please scroll down to see the full text article.

2003 J. Phys.: Condens. Matter 15 3855

(<http://iopscience.iop.org/0953-8984/15/23/302>)

View [the table of contents for this issue](#), or go to the [journal homepage](#) for more

Download details:

IP Address: 171.66.16.121

The article was downloaded on 19/05/2010 at 12:12

Please note that [terms and conditions apply](#).

# Numerical modelling of transport in a liquid diffusion couple shear cell

**Bing-Jian Yang and Reginald W Smith**

Materials Science and Microgravity Applications Group, Nicol Hall, Queen's University,  
Kingston, ON, K7L 3N6, Canada

E-mail: smithrw@post.queensu.ca

Received 27 January 2003

Published 30 May 2003

Online at [stacks.iop.org/JPhysCM/15/3855](http://stacks.iop.org/JPhysCM/15/3855)

## Abstract

A model is developed to explore some important issues, such as the effects of the rate of shear on the mixing of the liquid charges, the actual solute distribution at the start of the diffusion anneal period and the effect of a local reduction in liquid charge diameter on the measurement of a liquid diffusion coefficient. A numerical simulation with a grid sliding technique was used to simulate the movable computational domain. The computed results show that the shearing rate has only a small effect on the initial distribution of the solute at the moment when the two liquid columns become aligned, and that the region over which the solute concentration changes from that of the solvent charge to that of the solute-rich charge of the diffusion couple will be very narrow. However, the simulated results reveal that strong convection is produced due to shearing and that the disturbed region is much bigger than the zone over which the solute distribution is disrupted. The convection induced by shearing dissipates within 8 s after the termination of the shearing action for a shear cell with liquid column of 1.5 mm diameter and shear at rates of 4–40 mm s<sup>-1</sup>. The simulated results also indicate that a small void (approximately one-sixth of the diameter cross-section) in the liquid solvent near the sheared interface does not affect development of the initial solute concentration profile and its subsequent change with diffusion through the interface.

(Some figures in this article are in colour only in the electronic version)

## 1. Introduction

It is well known that diffusion transport in liquids continues to be an issue of fundamental interest. In order to measure or observe the inter-diffusion process, two different liquid charges need joining together. The diffusion coefficient in liquid is a key parameter to describe the diffusive mass transport rate, and it plays an important role in solidification, crystal growth,

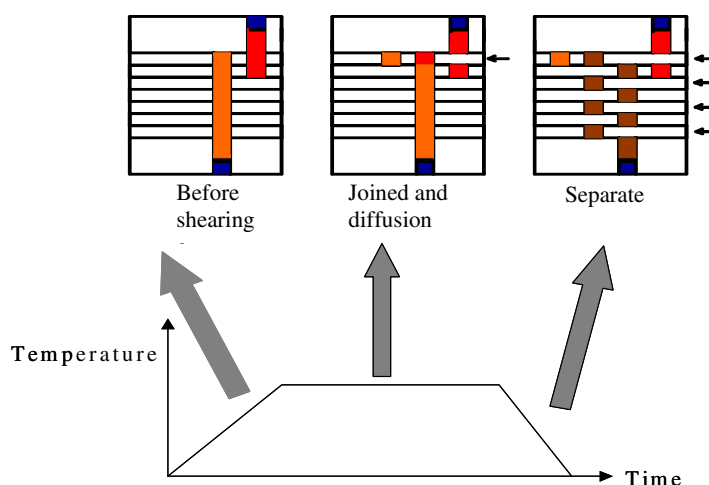


Figure 1. Shear cell operation and its time schedule.

glass formation and any modelling that involves mass transport. Although the diffusion coefficient in a liquid might be estimated with several existing models, none of them can give a satisfactory value for all temperature conditions. Therefore, the measurement of diffusion coefficients for metallic liquids is very necessary and always considered to be of importance. Diffusion coefficients measured terrestrially are liable to be contaminated by the buoyancy transport resulting from liquid density variations due to local changes in chemical composition and/or temperature. In view of this there is much interest in measuring diffusion coefficients in a reduced gravity environment, e.g. a lower orbiting space platform such as the NASA Shuttle or the International Space Station. Two kinds of experimental technique have been used to measure diffusion coefficients in the microgravity environment, i.e., the long capillary method and the shear cell method. The shear cell technique is very attractive and has some merits not possessed by the long capillary method; it also has some disadvantages. The shear cell technique has been used to measure liquid diffusion coefficients in molten metals [1, 2] and semiconductors [3, 4], as well as thermodiffusion, under microgravity conditions [5]. The entire process may be divided into four parts: joining, sharp stop, holding and the dividing processes. The shear cell method is demonstrated in figure 1. The shear cell configuration brings together clean sheared surfaces of the two liquids of the diffusion couple. In our recent design, the capillaries of each half of the diffusion couple are extended 3 mm past the diffusion junction. When the two parts of the diffusion couple are aligned at the beginning of the diffusion period, a 3 mm section is sheared off, creating a fresh face for each part of the diffusion couple and ensuring that no contaminants, such as bubbles, voids and oxide particles, are at the diffusion junction. Here the process from the moment at which the shearing starts to the moment at which the two liquid columns are aligned is called the joining process.

Although the shear cell method has many advantages, its initial condition for the diffusion measurement still deviates from an ideal one-dimensional transport condition. Obviously, we need to know how big this deviation will be, how strong any shear-induced convection in the liquid sample will be and its influence on the final solute distribution. These are important issues for shear cell designers and scientific investigators.

Jalbert *et al* [6] have numerically simulated the insensitivity of liquid diffusion measurements for the long capillary specimen in which the diffusion path is partially obstructed

by bubbles/voids or an oxide layer between the segments of a diffusion couple. They found that local obstructions to the transport path have to be in excess of half the transport path's cross-section to result in an apparent diffusivity  $D_a \leq 0.95D$ . Griesche *et al* [7] showed the error of the diffusion coefficient determination can be increased by shear convection. Mathiak *et al* [8] performed a numerical simulation to optimize the design and working parameters of the FOTON shear cell, but the simulation was done on the assumption of a time-dependent or constant tangential velocity boundary condition exerted on the ends of each liquid column; however, the mass exchange and corresponding transport of the species in the joining process from the start of shearing to the sharp-stop moment of its completion was not modelled. A similar modelling method was used by Arnold and Matthiesen [9] and Zeng *et al* [10]. Apparently, the existing methods cannot unveil the real initial conditions and the effect of shear convection on changes in solute distribution during shearing. An understanding of the optimization of the shear cell approach is very necessary in order to design and implement successful diffusion experiments on the ground and in space.

In this paper, we eliminate the assumptions of the effects of the shearing action on the ends of each liquid column and, instead, develop a new model to consider the mass exchange between two liquid columns during shearing, explore its influence on the conditions at the beginning of the diffusion anneal period on the solute concentration distribution and so define the real initial conditions from which the liquid diffusion coefficient may be calculated.

## 2. Model description

The actual shearing of the fluid columns in a shear cell is complex. As a first approximation, we assume a two-dimensional isothermal model and use it to simulate the rotating joining process of the two half liquid columns. A diameter of 1.5 mm is also assumed since it corresponds to the specimen size in our new design of shear cell, as shown in figure 1. The solute part is 3 mm long and the solvent part is assumed to be a semi-infinite cylinder with the first 6 mm length in our computational domain with a symmetrical boundary at the end. Although this particular model does not consider the effects of rotation in the space environment, the major features during shearing can be revealed. This is a very important step to better understand the mass mixing and species transport during the joining process, as well as the longer range effects of shear convection.

A Newtonian fluid with a constant kinematic viscosity and density is assumed, and solutally-driven buoyancy convection is assumed to be negligible. The Navier–Stokes equations in conjunction with mass and species transport are used to describe the transport phenomena. The finite volume method in the CFD computational package, CFX [11], is applied to solve the partial differential equations. The governing conservation equations for the isothermal process under microgravity ( $g \approx 0$ ) are

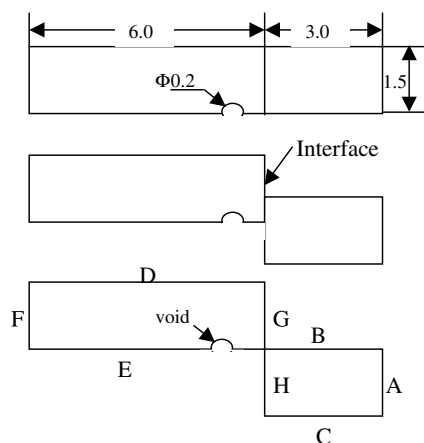
$$\nabla \cdot U = 0 \quad (1)$$

$$\rho \left( \frac{\partial U}{\partial t} + U \cdot \nabla U \right) = -\nabla P + \mu \nabla^2 U \quad (2)$$

$$\frac{\partial C}{\partial t} + U \cdot \nabla C = D \nabla^2 C \quad (3)$$

where  $t$  is time,  $P$  is pressure,  $\rho$  is density,  $\mu$  is dynamic viscosity,  $C$  is the mass fraction of solute,  $D$  is diffusivity and  $U$  stands for the velocity in  $x$  and  $y$  directions.

The grid sliding technique [11] is used to simulate the movable computational domain and mass mixing behaviour during shearing. The Pb–1 wt% Ag inter-diffusion couple is chosen and the diameter of the shear cell is 1.5 mm in accordance with our current shear cell design.



**Figure 2.** Schematic diagram of computational domain and physical conditions (A, B, C, D and E are no-slip walls, F is a symmetric plane and G and H are a sliding boundary).

The simulating conditions and the boundary conditions are demonstrated in figure 2. The viscosity is  $6.02 \times 10^{-3} \text{ kg m}^{-1} \text{ s}^{-1}$ , density is  $11\,340.0 \text{ kg m}^{-3}$  and diffusion coefficient of Ag in liquid Pb is  $1.022 \times 10^{-8} \text{ m}^2 \text{ s}^{-1}$  in all calculations.

Three dimensionless parameters are introduced for our discussion, i.e., the Reynolds number ( $Re$ ), the Schmidt number ( $Sc$ ) and the Peclet number based on the mass transport ( $Pe$ ). These dimensionless parameters are defined as follows:

$$Re = \rho V_{sr} d / \mu$$

$$Sc = \nu / D$$

$$Pe = Vd / D$$

where  $d$  is the diameter of the shear cell, which is 1.5 mm,  $V_{sr}$  is the shear rate and  $\nu$  is the kinematic viscosity ( $=\mu/\rho$ ).  $V$  is a characteristic velocity, and it takes  $V_{sr}$  for the joining process but takes a horizontal convective velocity obtained from the calculated result after the termination of the joining process.

The interface between the void and liquid is set to a no-slip wall without consideration of surface tension. The right-hand column of the shear cell is sliding from the moment at which the two liquid columns achieve contact to the moment at which the two columns are aligned. We call this period of sliding the ‘joining process’, and the moment of alignment of both halves of the diffusion couple we call the ‘initial condition’ for the measurement/calculation of the diffusion coefficient. The sliding boundary marked at G and H in figure 2 is a permeable interface.

### 3. Case study and discussion

The model to be developed will explore the effect of shear convection, the actual initial condition and the effect of column diameter restrictions or defects on the measurement of the liquid diffusion coefficient. The following cases will be investigated:

- (1) a case without any defects, and shear at a small shear rate of  $4 \text{ mm s}^{-1}$ ;
- (2) a case with a void (see figure 2), and shear at a small shear rate of  $4 \text{ mm s}^{-1}$ ;
- (3) a case without a void and with shear rate  $20 \text{ mm s}^{-1}$ ;
- (4) a case without any defects, and shear with a large shear rate of  $40 \text{ mm s}^{-1}$ ;
- (5) a case with a void, and a shear rate of  $40 \text{ mm s}^{-1}$ .

**Table 1.** Variations of dimensionless parameters with shear rate.

$V_{sr}$ (mm s <sup>-1</sup> )	$Re$	$Pe$	$Sc$
4	11.3	587	52
20	56.5	2935	52
40	113.0	5870	52

The variation of the dimensionless parameters for these three shear rates is demonstrated in table 1 for the joining process. Note that the maximum velocity in the axial direction is used as the characteristic velocity to estimate the mass  $Pe$  number after the termination of the shearing process.

The computed results at shear rates of 4, 20 and 40 mm s<sup>-1</sup> are shown below. When the joining stage is finished and the diffusion couple is formed, the sample is then annealed for the solute to diffuse for a given time. The following issues will be discussed, taking note of the computed results. Note that in all tables and figures the velocity at any position is referenced to the initial stationary frame and not to that of the moving grid.

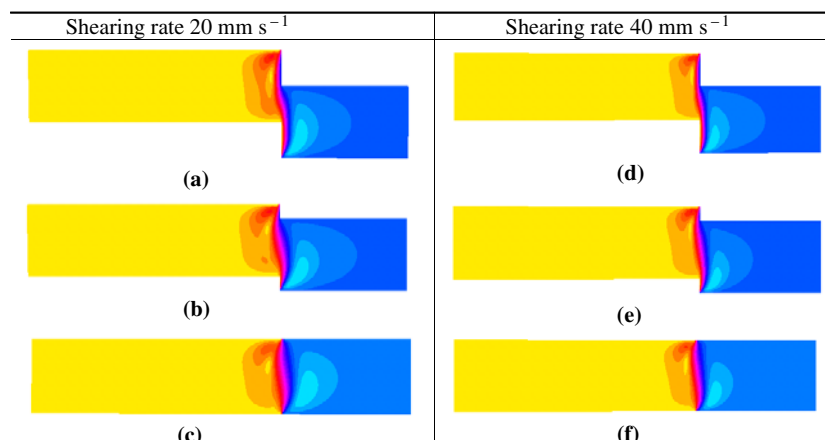
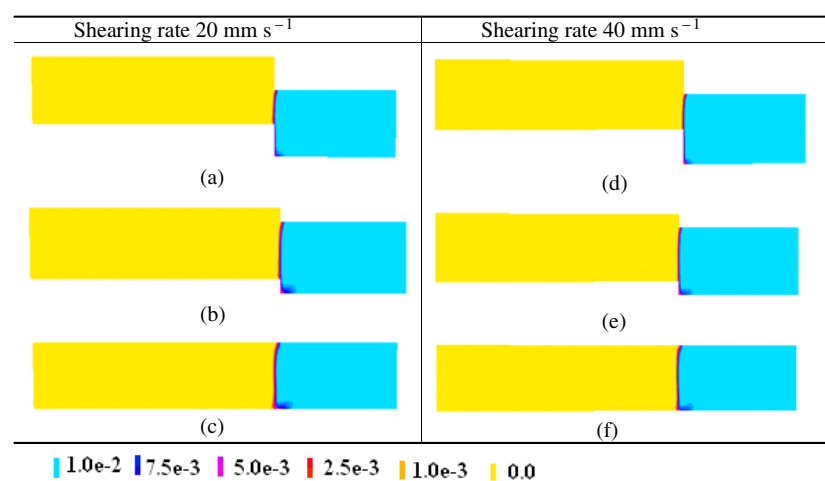
### 3.1. The behaviour during the joining process

The cases with shear rates of 20 and 40 mm s<sup>-1</sup> are chosen to explore the momentum and species transport phenomena during the joining process, as shown in tables 2 and 3. During joining, the shearing liquid drags the stationary liquid along with it due to the internal friction, but the disrupted depth of the convective region is limited to within the size of only one column diameter during the joining. It is worthwhile to notice that the disrupted zone of solute distribution at a given moment is quite different to that of the disturbed region of shear convection. This is because the rate of the mass exchange during joining is much slower than that of momentum transport in a viscous liquid. Here  $Sc = 52$  and  $Pe = 2935$ – $5871$ . Some of the dilute alloy (1 wt% Ag) is brought into the solvent liquid, but the amount is very small. The solute mixing at the moment when the two charges are aligned is also limited for the shear rates of 4, 20 and 40 mm s<sup>-1</sup> (see table 5). The narrow and flat pattern for the distribution of solute is our expected result for the initial condition of the shear cell. The ideal condition is one where the solute concentration has a sharp discontinuity at the interface between the two liquid columns.

Furthermore, it is found that, for a given point in the joining process, there is no obvious difference in the size and shape of the disturbed region of convection for the three cases considered, and neither is the solute concentration distribution significantly different.

### 3.2. Effect of shear rate




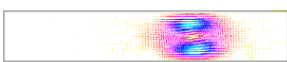

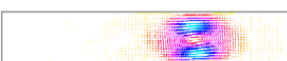

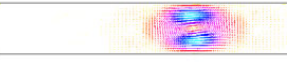

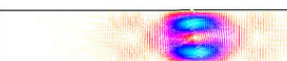
The shear rate is one of the major variables in shear cell design and strongly links with the intensity of shear convection. It can be seen from tables 3–5 that the shear rate has little effect on the initial distribution of the velocity vector and disturbed region of convection, but affects somewhat the solute distribution at the moment when the two liquid columns just complete the joining process. This is a result of different contact times and orientation of mass transport. Although the mass  $Pe = 587$ – $5870$  during the joining process, the mass transport along the axial direction is more dependent upon the momentum transport in the same direction. The maximum mass  $Pe$  number in the axial direction during the joining process is of the order of 10 or less based on the computed results. Thus, the non-uniform solute distribution

**Table 2.** Convectively disturbed region during the joining process for different shearing rates.**Table 3.** Distribution of solute during the joining process for different shearing rates.











(disrupted zone) is very narrow around the interface between the solvent and the solute-rich solution. However, the simulated results revealed that two counter-flow whirlpools exist due to shearing and that these whirlpools move away from the interface, so that the depth of the disturbed region in the velocity field is less than one column diameter during the entire joining process.

As discussed earlier for the joining process, although the convective penetration length in the solvent charge is less than one column diameter, it is much larger than the disrupted region of the solute concentration in the solvent charge. This can be partially explained with the  $Sc$  number shown in table 1.  $Sc = 52$  means that the momentum diffusivity is 52 times larger than the mass diffusivity. Tables 2 and 3 show how the shearing process influences the solute concentration profile through the joining plane at three times following the moment when the two charges become fully aligned. Let us now consider the following cases: case (1), the moment the charges are aligned; case (2), 1 s after start of shear; case (3), 2 s after start of shear, and case (4) 16 s after start of shear.

**Table 4.** Velocity fields for various conditions.

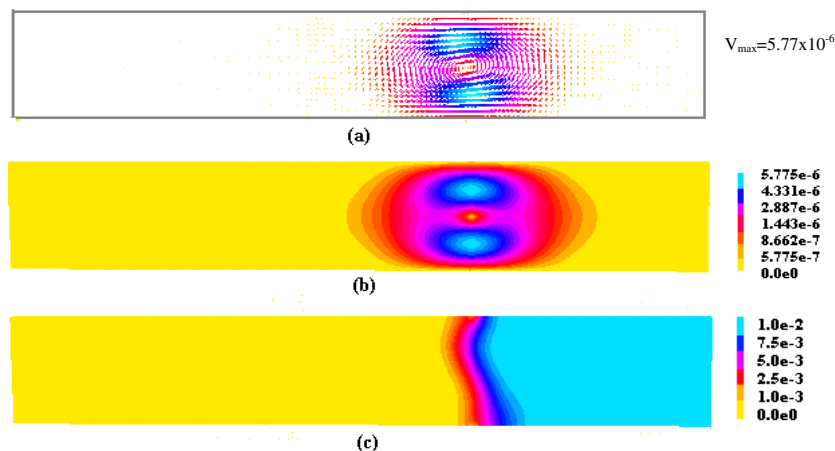
Shear rate mm s <sup>-1</sup>	Void	Velocity vector at moment aligned	Velocity vector at 1.0 s after starting to shear
4	yes	 (a)	 (f)
4	no	 (b)	 (g)
20	no	 (c)	 (h)
40	no	 (d)	 (i)
40	yes	 (e)	 (j)

**Table 5.** Variations of convective penetration length and concentration distribution at the joining moment under different conditions.

Shear rate mm s <sup>-1</sup>	Void	Disturbed region and V <sub>max</sub> at joining moment	Concentration pattern at joining moment
4	yes	 $V_{\max} = 4.270 \times 10^{-3} \text{ m s}^{-1}$ (a)	 (f)
4	no	 $V_{\max} = 4.249 \times 10^{-3} \text{ m s}^{-1}$ (b)	 (g)
20	no	 $V_{\max} = 2.268 \times 10^{-2} \text{ m s}^{-1}$ (c)	 (h)
40	no	 $V_{\max} = 4.637 \times 10^{-2} \text{ m s}^{-1}$ (d)	 (i)
40	yes	 $V_{\max} = 4.691 \times 10^{-2} \text{ m s}^{-1}$ (e)	 (j)

*Case 1.* A comparison of figures (c) and (f) in table 2 shows that the shear-induced convective penetration on either side of the joining plane is larger at 20 mm s<sup>-1</sup> shear rate than at





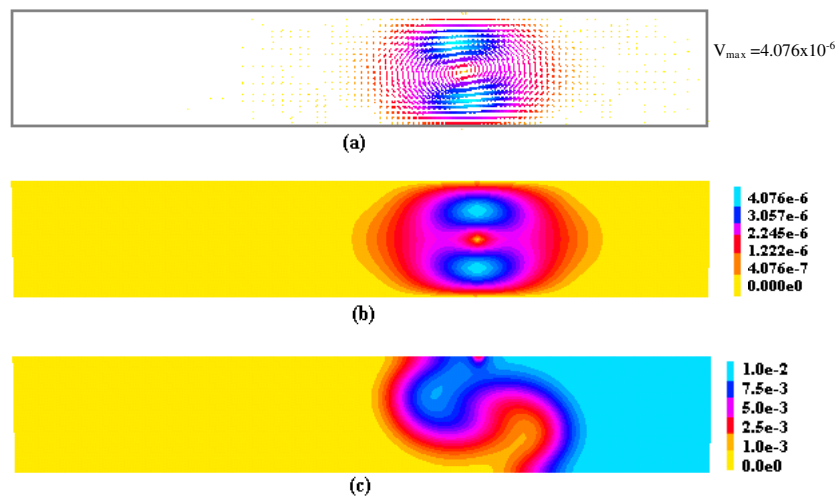
**Figure 3.** Computed results for the case with  $4 \text{ mm s}^{-1}$  shear rate at 2 s after the start of shear: (a) velocity vector; (b) convective disturbed zone; (c) solute concentration distribution.

$40 \text{ mm s}^{-1}$ . However, a comparison of figures (c) and (f) in table 3 suggests that the solute concentration at the start of the shearing process has suffered little change during shearing, i.e., the shear-induced convective flows have not appreciably altered the initial solute concentration profile of the diffusion couple. Table 5 gives data for shear rates of 4, 20 and  $40 \text{ mm s}^{-1}$ . It is seen that at the minimum shear rate of  $4 \text{ mm s}^{-1}$  the solute concentration has been rather more disturbed than at the larger shear rates, but even in this case, the distance over which the disturbance has taken place is small compared with the distance over which convective flows have been induced.

*Case 2.* 1 s after the start of shear: it is seen in table 4 that the patterns of induced flow are similar for these shearing rates, namely two counter-flow whirlpools, one at the top and the other at bottom of the shear plane. We have already shown that the mass Peclet number in table 1 does not reflect the relative mass transport rate in the axial direction. This velocity in the axial direction is small during the joining process, but becomes large after the termination of the joining process. At 1 s after the start of shear, the  $Pe$  number for the maximum velocity in the axial direction is 2.97 for  $4 \text{ mm s}^{-1}$  shear rate, 1.4 for  $20 \text{ mm s}^{-1}$  and 1.2 for  $40 \text{ mm s}^{-1}$ . Therefore, the mass transport in the axial direction induced by shear convection is significant, and the larger the shear rate, the more mass transport along the axial direction after the shearing stops.

*Case 3.* 2 s after the initiation of the shearing process: the counter-flow whirlpools for the two shear rates appear to be similar in shape but the fluid velocities are very different. These counter-flow whirlpools have now caused the joining plane to become convoluted (figures 3 and 4); however, whilst the scale of the convolution is relatively small for the  $4 \text{ mm s}^{-1}$  shear rate (figure 3), it becomes as large as that of the fluid flow in the case of the specimen subjected to the  $40 \text{ mm s}^{-1}$  shear rate (figure 4). At 2 s after the initiation of the shearing process,  $Re = 11.3$  and  $Pe = 0.85$  in the axial direction for  $4 \text{ mm s}^{-1}$  shear rate and  $Re = 113.0$  and  $Pe = 0.6$  in the axial direction for  $40 \text{ mm s}^{-1}$  shear rate.

It is interesting to compare more closely figures 3 and 4. Whilst the patterns of flow induced by shearing at 4 and  $40 \text{ mm s}^{-1}$  appear to be similar (figures 3(b) and 4(b)), the



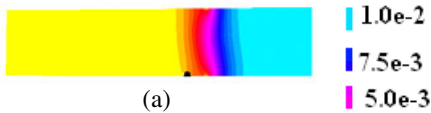
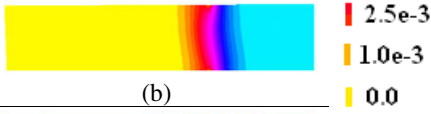
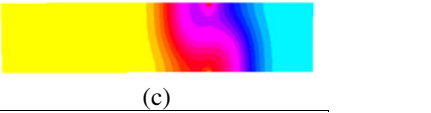
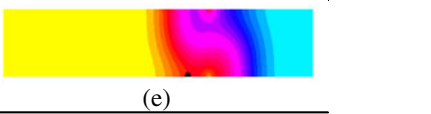
**Figure 4.** Computed results for the case with  $40 \text{ mm s}^{-1}$  shear rate at 2 s after the start of shear: (a) velocity vector; (b) convective disturbance zone; (c) solute concentration distribution.

patterns for solute concentration are very different (figures 3(c) and 4(c)). The maximum velocity in figure 3 is  $5.775 \times 10^{-6} \text{ m s}^{-1}$ , which is greater than the velocity in figure 4 ( $4.076 \times 10^{-6} \text{ m s}^{-1}$ ); in view of this it might appear strange that figure 4 shows the effects of considerably more local mixing and so the region must have been subject to much more fluid flow. The answer to this apparent contradiction is the fact that whilst the act of shearing takes approx  $0.375 \text{ s}$  in the case of the  $4 \text{ mm s}^{-1}$  shear rate, this operation would take only  $0.0375 \text{ s}$  when shearing takes place at  $40 \text{ mm s}^{-1}$  and hence, at the elapsed time of 2 s after the initiation of shearing, the induced flow in the  $40 \text{ mm s}^{-1}$  shearing rate will have had more time to affect the solute distribution and so produce the effect shown in figure 4(c). In fact, if we examine the situation at the interface just after completion of the joining process between two columns, the maximum velocity would be found to be about ten times higher in the case of  $40 \text{ mm s}^{-1}$  shear rate than that in the case of  $4 \text{ mm s}^{-1}$ , as shown in table 5. At the moment of alignment, the mass  $Pe = 6885$  for  $40 \text{ mm s}^{-1}$  and  $626$  for  $4 \text{ mm s}^{-1}$ . Thus, stronger mass transport results from the momentum transport induced by shearing operation in the case of  $40 \text{ mm s}^{-1}$  shear rate.

*Case 4.* 16 s after start of shear: we note that the shear-induced fluid flows had completely dissipated within the first 8 s after the initiation of shear at  $4 \text{ mm s}^{-1}$ , and probably in 2 s at the  $40 \text{ mm s}^{-1}$  shear rate, so the solute concentration distributions shown in table 6 reflect the effects of the flow and also the purely diffusive mass transport until 16 s. It is seen that whilst the originally sharp interface between the alloy charge and solvent charge has become broader, particularly for the larger shear rate, the presence of a small discontinuity in the solvent charge does not have any appreciable effect on the solute concentration profile.

In this analysis, we have assumed that convection is negligible if maximum velocity is less than  $10^{-7} \text{ m s}^{-1}$ . Thus we conclude that the contribution of shear convection to the solute transport will be limited to a very small part of the diffusion anneal period even for a short anneal period for a  $1.5 \text{ mm}$  specimen diameter shear cell.

**Table 6.** Variations of concentration under different conditions.

Shear rate $\text{mm s}^{-1}$	Void	Concentration pattern 16 s after start of shear
4	yes	 (a)
4	no	 (b)
40	no	 (c)
40	yes	 (e)

### 3.3. Effect of a discontinuity

A void is a defect that might exist in a diffusion couple. It could be a gas bubble or inclusion. If the void is considered as a gas bubble, then Marangoni forces due to solute gradients on the free surface could play a role in transporting the solute species, as shown in our earlier study of the effect of Marangoni convection on the hot tearing tendency of cast metals [12]. Because of the lack of data about the relationship of surface tension with solute concentration for the materials used for the diffusion couple, the void is assumed to be a solid inclusion with a non-penetration and non-slip interface. Two different shear rates, 4 and 40  $\text{mm s}^{-1}$ , were considered for shear cell operation. The size and position of the void is shown in figure 2. Comparisons of the computed results for fluid flow induced by shearing and solute concentration are shown in tables 5 and 6.

It can be seen that when a 0.2 mm hemispherical discontinuity exists, and is located at 0.55 mm from the interface plane between the solute-rich and solvent charges, the concentration distribution is similar to the case without a void. The penetration length and disturbed region due to shear convection for both cases under the same shear rate are almost identical at the moment of joining and at 16 s after the start of shearing.

The computed results for a time before 16 s, for instance, at the termination of the joining process shown in table 5, still fits this conclusion. Thus, a small void under the current situation does not affect the initial and subsequent patterns of solute concentration, even with a difference in the initial convection patterns induced by differences in shear rate.

## 4. Conclusions

A new model that includes the mass exchange during the joining process has been developed for the shear cell currently under development at Queen's University. Several cases have been simulated to explore the effects of shear convection and the presence of a void on the distribution of solute. The following conclusions are obtained.

- (1) The mass exchange during the joining process is limited, and the disrupted zone in the solute distribution profile is much smaller than the region of convection induced by

shearing. Because the Schmidt number,  $Sc$ , is 52 in our case, the momentum diffusivity is much greater than mass diffusivity.

- (2) The shear convection produces whirlpool circulations in the liquid, but significantly affects the solute distribution only in the very early stages from the initiation of shear for a shear cell with a diameter of 1.5 mm. The convective circulations greater than  $10^{-7} \text{ m s}^{-1}$  dissipate within 8 s after the completion of the joining process.
- (3) A small void near the interface does not show a significant influence on the initial solute concentration distribution and the subsequent diffusion pattern.
- (4) The shear rate affects the initial condition of concentration somewhat, but not significantly. The patterns at the moment of joining are almost identical for shear operations with rates of 20 and 40  $\text{mm s}^{-1}$ . The mass  $Pe$  during the joining process is much greater than that after alignment of the two liquid columns.

### Acknowledgment

This work is sponsored by the Canadian Space Agency (CSA).

### References

- [1] Kohl J G and Predel B 1978 *Z. Metallk.* **69** 248
- [2] Bourret E D, Favier E F and Bourrel O 1981 *J. Electrochem. Soc.* **128** 2437
- [3] Brauer P 1995 *PhD Thesis* Fakultat fur Physik, TH Karlsruhe (in German)
- [4] Kossler R 1990 *PhD Thesis* Fakultat fur Physik, TH Karlsruhe (in German)
- [5] Praizey J P 1987 *Proc. 6th Eur. Symp. on Material Science under g Conditions (Bordeaux, 1986)* SP-256 ESA p 501
- [6] Jalbert L B, Rosenberger F and Banish R M 1998 *J. Phys.: Condens. Matter* **10** 7113
- [7] Griesche A, Kraatz K-H, Froberg G, Mathiak G and Willnecker R 2000 *Proc. ESA Mtg (Sorrento, 2000)* p 497
- [8] Mathiak G, Froberg G and Arnold W A 1997 *Proc. Fluid in Space 2 (Naples)* p 396
- [9] Arnold W A and Matthiesen D 1995 *J. Electrochem. Soc.* **142** 433
- [10] Zeng Z, Mizuseki H, Ichinoseki K and Kawazoe Y 1998 *Numer. Heat Transfer A* **34** 709
- [11] 2001 *User Manual for CFX4.4* AEA Technology
- [12] Yang B J, Smith R W, Sahoo M and Sadayappan M *AFS Trans.* **110** 375–81